ELSEVIER

Biophysical Chemistry 87 (2000) 167–178

Biophysical Chemistry

www.elsevier.nl/locate/bpc

Electromigration of polyion homopolymers across biomembranes: a biophysical model

Teresa Janas[a], Henryk Krajiński[b], Tadeusz Janas[b,*]

[a] *Department of Physics, Technical University, Podgórna 50, 65-246 Zielona Góra, Poland*
[b] *Department of Biophysics, Pedagogical University, Monte Cassino 21 B, 65-561 Zielona Góra, Poland*

Received 26 December 1999; received in revised form 25 June 2000; accepted 20 July 2000

Abstract

The analysis of polyion transmembrane translocation was performed using membrane electrical equivalent circuit. The dependence of polyion flux across membranes on time, membrane electrical conductance, membrane electrical capacitance, degree of polymerization, water solution conductance and applied transmembrane potential is discussed. The changes in polyion flux were up to 88% after 1 ms. Both the increase of polyion chain length and the decrease of membrane conductance resulted in the diminution of this effect. Inversion of flux direction was observed as a result of external potential changes. Reversal curves, representing the values of considered parameters for zero-flux were also shown. The replacement of a polyanion by a polycation of the same chain length resulted in the same shape of the surface plot but with opposite orientation. The analysis describes the effect of transmembrane potential on the translocation rate of polyanionic polysialic acid and polynucleotides, and polycationic peptides across membranes.

Keywords: Polysialic acid; Membrane transport; Polyanion flux; Polycation flux; Electrical equivalent circuit

1. Introduction

Polysialic acid (polySia) chains are linear homopolymers (the degree of polymerization $D = \sim 8-200$) of α-2,8-linked sialic acid [1]. The valency of this polyanion corresponds to the degree of polySia polymerization. The minimum chain length of polySia reflects characteristic formation of a helical conformation [2]. In neural cells polySia is attached to neural cell adhesion molecule (NCAM), the only confirmed cell surface polySia carrier in vertebrates, through a developmentally regulated process. PolySia is able to attenuate adhesion forces and modulate overall cell surface interactions, thereby orchestrating

* Corresponding author. Tel.: +48-68-323-4080; fax: +48-68-326-5449.
E-mail address: tjanas@asia.aw.wsp.zgora.pl (T. Janas).

0301-4622/00/$ - see front matter
PII: S0301-4622(00)00189-7

dynamic changes in the shape and movement of cells, as well as their processes [3]. The concentration of polySia at the cell surface results from the combination of several regulatory mechanisms. One is biosynthesis, which probably depends on the level of transcription and/or activity of the polysialyltransferase. The other mechanisms are biosynthesis independent. They involve intracellular trafficking to and from the cell surface, as well as degradation. It can be speculated that the latter processes result in rapid changes of polySia surface expression, whereas changes in biosynthesis would be observable only after longer periods of time [3].

PolySia chains constitute a structurally unique group of carbohydrate residues that covalently modify surface glycoconjugates on cells that range in evolutionary diversity from bacteria to human brains [4,5]. Expression of the polySia capsule on the surface of neuroinvasive *Escherichia coli* K1 and *N. meningitidis* serogroup B and C cells is important in pathogenesis, since it appears to facilitate bacterial invasion and colonization of the meninges in neonates. The capsule in *E. coli* K1 strains is a receptor for polySia specific bacteriophages that require expression of the capsule for infectivity [4,5]. The degree of polymerization of polySia in bacterial cells can extend beyond 200 polySia residues [6]. PolySia is an oncodevelopmental antigen in human kidney and brain, and may enhance the metastatic potential of Wilms tumor cells and neuroblastomas [3]. These novel carbohydrate chains also appear to have a regulatory role in cell growth, differentiation, fertilization and neuronal pathogenicity [3]. Studies on the function of polySia suggest that its primary role is to promote developmentally controlled and activity-dependent plasticity in cell interactions and thereby facilitate changes in the structure and function of the nervous system [7]. PolySia appears also to be an important regulatory element in neural plasticity, nerve regeneration and as an oncofetal marker on tumor cells [7]. Although a lot of surface molecules regulate cell-cell interactions, polySia appears unique both in its simple structure and in the multitude and complexity of events it might control [3].

The transmembrane translocation of polySia chains across the inner membrane of *E. coli* K1 bacterial cells requires both the membrane protomotive force and the transmembrane electrical potential gradient [4,5]. The genes encoding proteins necessary for synthesis and expression of the polySia capsule in *E. coli* K1 have been cloned and characterized [8]. In *E. coli,* the 12–14 genes required for these processes are located in a multiple *kps* cluster. The 17 kb *kps* cluster is divided into three functional regions [9]. The central region 2 contains the information for synthesis, activation and polymerization of sialic acid. Region 3 genes are postulated to be involved in transport of polySia across the bacterial inner membrane while region 1 genes appear to function in the transport of polymers to the external surface of the outer membrane. In the present paper the analysis of polySia translocation across the inner membrane in *E. coli* K1 has been performed using the method of the electrical equivalent circuit of the membrane. The theoretical study presents a dependence of polyanion flux through membrane on time, membrane electrical conductance, membrane electrical capacitance, degree of polymerization, water solution conductance and applied transmembrane potential. The derivation is based on the equivalence electrical circuit of the investigated system. The calculations and graphs were done using the Mathematica (Wolfram Research, Inc.) computational program. A similar study was also performed for polycationic homopolymers.

2. Theory

Hodkin and Huxley used an equivalent circuit and Ohm's law to derive a relationship between total membrane current and the membrane capacitance, the membrane voltage, the time, ion and leakage conductances, the equilibrium potentials for each of the ions, which they applied to nerve signaling [10]. Attempts to modify the Hodkin–Huxley equations have met with limited success. In order to include the effects of an electrogenic ion pump on the membrane potential Mul-

lens and Noda added a factor to the Goldman equation [11]. Modifications of the Hodkin–Huxley equation have been applied to solve for membrane voltage in the presence of electrogenic pumps [12]. Non-equilibrium thermodynamics have been used to analyze transport in animal cells [13]. Martin and Harvey applied ionic circuit analysis to examine transport in lepidopteran midgut components [14]. In their analysis the concept of electrical equivalent circuit for membrane was extended to include components found in membrane ionic transport systems. Each of the electrical components represented a corresponding physical component in the membrane systems: capacitors represented the plasma membrane with its insulating lipid core separating two conductive aqueous solutions, resistors represented the various ionic channels found in the membrane, batteries represented energy sources driven by chemical reactions or ionic gradients having an electromotive force (emf) equal to the corresponding Nernst equilibrium potential. Ideal batteries have a constant output potential determined by the free energy of the chemical reaction. In the case when the internal resistance is in series with an idealized battery and the battery discharges, the open-circuit potential of the battery remains constant whereas the closed-circuit output voltage decays. The models, having the form of equivalent electrical circuits, can be subjected to standard electrical circuit analysis techniques to describe quantitatively the voltage and current relationships among the components. These fundamental techniques of circuit analysis include Ohm's law and Kirchhoff's laws. Pumps are special cases of porters and the input side of a pump can be driven by the free energy, the pump potential, expressed in volts of the chemical reaction (e.g. ATP hydrolysis) [15]. Viewing the energy distributions in membranes as the functions of the voltage, current, capacitance and resistance parameters of the pumps, channels, membranes and compartments of the system presents an opportunity to use computer programs. These programs allow study of how different circuit configurations can quantitatively affect the operation of a system.

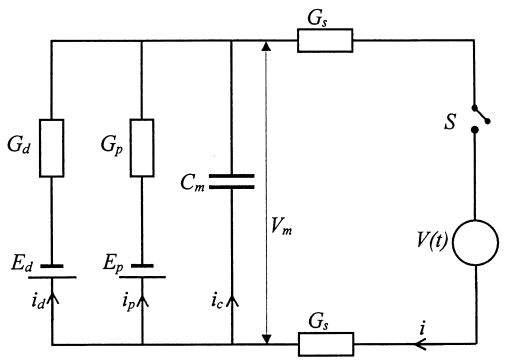

Fig. 1. The equivalent electrical circuit of a biomembrane, where: G_p ($\Omega^{-1}\cdot cm^{-2}$) is the electrical conductance of the ion pump; G_d ($\Omega^{-1}\cdot cm^{-2}$) is the electrical conductance of the membrane for the diffusion process; G_s ($\Omega^{-1}\cdot cm^{-2}$) is the electrical conductance of the bathing solution and the electrodes; E_d (V) is the diffusion potential; E_p (V) is the electromotive force of ion pumps; i ($A\cdot cm^{-2}$) is the total current; i_d ($A\cdot cm^{-2}$) is the diffusive current; i_p ($A\cdot cm^{-2}$) is the current passing through the pumps; i_c ($A\cdot cm^{-2}$) is the capacitive current per the surface unit; V_m (V) is the electrical potential of the membrane; C_m ($F\cdot cm^{-2}$) is the capacitance of the membrane; $V(t)$ (V) is the external potential source. The switch, S, closes the circuit at the time $t = 0$.

3. Derivation of the flux equations

The electrical equivalent circuit of the membrane is presented in Fig. 1. The left-hand branch of the circuit represents the passive diffusion of ions across the membrane; the membrane resistance (G_d^{-1}) is connected in series with the electromotive force (E_d) which is equivalent to the diffusion potential. The next (going to the right) branch represents the electrogenic pumps which actively transports ions out of the cell; G_p is the total conductance of the electrogenic pumps located in the membrane; E_p is the electromotive force of the electrogenic pumps. C_m, G_s and $V(t)$ represent the membrane capacitance, the electrical conductance of the bathing solution and the electrodes, and the external potential source, respectively. The switch, S, closes the circuit at the time $t = 0$. From the first Kirchhoff's law we have:

$$i = i_d + i_p + i_c \quad (1)$$

where i ($A \cdot cm^{-2}$) is the total current, i_d is the diffusive current, i_p is the current passing through the pumps, i_c is the capacitive current (all currents per unit area).

The currents can be calculated from Ohm's laws:

$$i_d = G_d(V_m - E_d)$$

$$i_p = G_p(V_m - E_p)$$

$$i_c = C_m \frac{dV_m}{dt} \tag{2}$$

where t (s) is time, G_d ($\Omega^{-1} \cdot cm^{-2}$) is the electrical conductance of the membrane resulting from diffusion process, E_d (V) is the diffusion potential, G_p ($\Omega^{-1} \cdot cm^{-2}$) is the electrical conductance of ion pumps, E_p (V) is the electromotive force of ion pumps, C_m ($F \cdot cm^{-2}$) is the capacitance of the membrane, V_m (V) is the electrical potential of the membrane.

After inserting Eq. (2) into Eq. (1) we obtain:

$$i = G_d(V_m - E_d) + G_p(V_m - E_p) + C_m \frac{dV_m}{dt} \tag{3a}$$

and after transforming:

$$i = V_m(G_d + G_p) - (G_d E_d + G_p E_p) + C_m \frac{dV_m}{dt} \tag{3b}$$

The electrical conductance of the membrane G_m ($\Omega^{-1} \cdot cm^{-2}$) can be presented as:

$$G_m = G_d + G_p \tag{4}$$

In the case, when the membrane potential, V_m, equals to the resting potential, E_r, the current passing through the membrane $i_r = i_d + i_p$. Therefore:

$$E_r G_m = G_d E_d + G_p E_p \tag{5}$$

The resting state of the membrane ($V_m = E_r$) is represented by the switch, S, in the 'open circuit' position. Combining Eqs. (3b)–(5) we get:

$$i = V_m G_m - E_r G_m + C_m \frac{dV_m}{dt} \tag{6}$$

From the second Kirchhoff's law:

$$V = V_m + 2V_s \tag{7}$$

where V (V) is the external potential, V_s (V) is the drop of the electrical potential on the electrical resistance, R_s (Ω), of the bathing solution and electrodes.Therefore:

$$V_m = V - \frac{2i}{G_s} \tag{8}$$

where G_s [$\Omega^{-1} \cdot cm^{-2}$] is the electrical conductance of the bathing solution and the electrodes, $G_s = 1/R_s = i/V_s$.

After inserting Eq. (8) into Eq. (6) and rearranging we get:

$$i\left(1 + \frac{2G_m}{G_s}\right) + \frac{2C_m}{G_s} \cdot \frac{di}{dt} = G_m V - E_r G_m + C_m \frac{dV}{dt} \tag{9}$$

Since $i = JzF$, where J ($mol \cdot s^{-1} \cdot cm^{-2}$) is the ion flux through membrane, z is the ion valency, $F = 9.65 \times 10^4$ ($C \cdot mol^{-1}$) is the Faraday's constant, we obtain:

$$J\left(zF + \frac{2zFG_m}{G_s}\right) + \frac{2C_m zF}{G_s} \cdot \frac{dJ}{dt} = G_m V - E_r G_m + C_m \frac{dV}{dt} \tag{10}$$

After substituting for:

$$A = zF + \frac{2zFG_m}{G_s} \quad \text{and} \quad B = \frac{2C_m zF}{G_s}$$

we can write Eq. (10) in the form:

$$AJ + B\frac{dJ}{dt} = G_m V - E_r G_m + C_m \frac{dV}{dt} \tag{11}$$

Eq. (11) represents a first order differential equation. This equation have been solved for $V = V_0$ (the electrical potential source, $V(t)$, keeps the external potential, V, at the level V_0) for the initial condition, $J(t=0) = J_0$:

$$J(t) = \frac{G_m(V_0 - E_r)}{A} + \left[J_0 - \frac{G_m(V_0 - E_r)}{A}\right] e^{-(A/B)t} \qquad (12)$$

Eq. (12) describes the unidirectional flux of polyions across the membrane. In this paper we used Eq. (12) to analyze the relationship between the flux of polyion chains across the membrane and the variables as: membrane conductance, membrane capacitance, polyion degree of polymerization, external potential and time.

4. Results and discussion

The membrane-associate polysialyltransferase complex in *E. coli* K1 catalyses the synthesis, transmembrane translocation and assembly of capsule polymers containing α-2,8-ketosidically linked polySia. To determine the molecular mechanism of the translocation of sialyl polymers across the inner bacterial membrane, an in vivo system was developed [4,5] which used spheroplasts prepared from *E. coli* K1 cells that are unable to degrade sialic acid (nanA4 mutation). PolySia chains that have been translocated across the inner membrane were differentiated from those chains remaining inside by their sensitivity to depolymerization by endoneuraminidase. After pulse-labeling the spheroplasts with ^{14}C-Neu5Ac, synthesis and translocation were followed kinetically and the theory of compartmental analysis was applied for determination of polySia distribution between different compartments. The studies showed that both $\Delta\mu_H$ and $\Delta\psi$ are actively involved in the transmembrane translocation of polySia and suggest that the relatively large transmembrane electrical potential gradient, up to -150 mV (negative inside), that is generated across the *E. coli* inner membrane, may facilitate the movement of these polyanions across the membrane.

In this study we used the electrical equivalent circuit analysis in order to present a biophysical model of the observed by us in [4,5] modulation of polySia transmembrane translocation rates by the ionophores. Eq. (12) derived in Section 2 have been used for plotting three-dimensional graphs. The value of $J_0 = 5 \times 10^{-17}$ mol·s^{-1}·cm^{-2} (the number of moles of polySia translocated (s^{-1} cm^{-2}) of the inner membrane surface of bacterial cells) was calculated from the polySia biosynthesis rate [16] and from the number of polySia chains per one bacterial cell estimated in [17].

Plots, showing the flux as a function of the degree of polyion polymerization are symmetrical with respect to the symmetry line perpendicular to the *DP* axis and passing through the point $J = J_0$ on the flux axis. The replacement of a polyanion by a polycation of the same chain length resulted in the same shape of the obtained surface plot but with opposite orientation. Fig. 2a and Fig. 3a show the transmembrane flux, J, of polySia chains as a function of the external potential, V_0, and time, t, or the external potential and the degree of polyion polymerization, *DP*, respectively. The graphs were plotted for the level of the membrane conductance equal to 10^{-6} Ω^{-1}·cm^{-2} and for the level of external potential equal to -0.06 V. The value of -0.06 V for the external potential was chosen in order to reflect the mean effect of applied ionophores to the bacterial spheroplast on the membrane potential of the cytoplasmic membrane [4,5]. PolySia is represented by negative values of *DP* which correspond to the polySia ionic valency. The reversal curves (Fig. 2b and Fig. 3b) calculated for the relationships in Fig. 2a and Fig. 3a, respectively, represent the critical values of external potential, time and the degree of polymerization for the case the polySia flux equals zero. As it can be evaluated from Fig. 2a, there is a 37% increase of the polySia flux (for $V_0 = -0.3$ V) from 5×10^{-17} mol·s^{-1}·cm^{-2} to 6.85×10^{-17} mol·s^{-1}·cm^{-2} after time $t = 1$ ms. After time $t = 1$ s there is an over 118-fold increase in the polySia flux, up to the value 5.91×10^{-15} mol·s^{-1}·cm^{-2}. In the case the external potential having a positive value 0.3

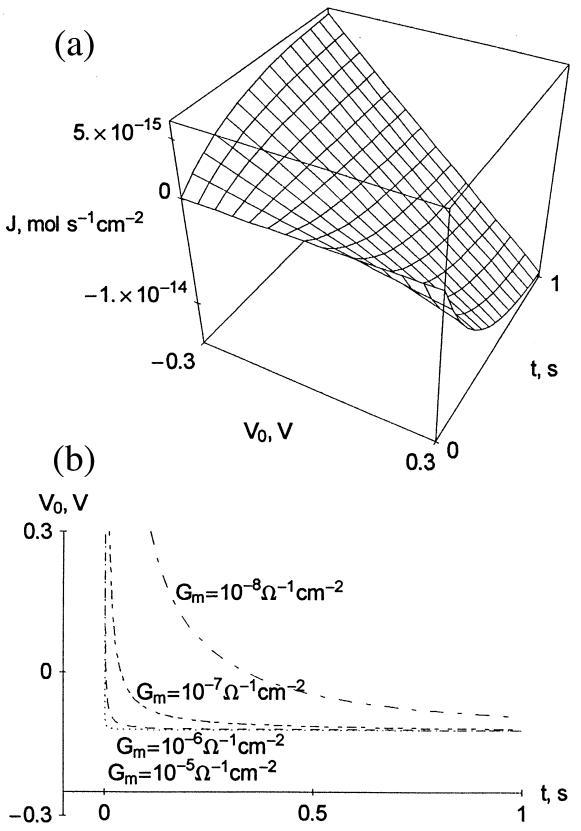

Fig. 2. (a) The dependence of the flux of polyion chains across the membrane, J, on the external potential, V_0, and time, t. Calculated for: the resting potential of membrane, $E_r = -0.12$ V; the electrical conductance of the bathing solution and the electrodes, $G_s = 10^{-6}\ \Omega^{-1}\cdot cm^{-2}$; the capacitance of membrane, $C_m = 5\times10^{-7}\ F\cdot cm^{-2}$; the electrical conductance of membrane, $G_m = 10^{-6}\ \Omega^{-1}\cdot cm^{-2}$; the degree of the polyion polymerization, $DP = -100$; the initial flux, $J_0 = 5\times10^{-17}$ mol·s^{-1}·cm^{-2}. (b) The reversal curves obtained from (a) and showing the relationship between the external potential, V_0, and time, t, for the polyion flux, $J = 0$. Each line was plotted for different electrical conductance of the membrane, G_m. Calculated for: the resting potential of the membrane, $E_r = -0.12$ V; the electrical conductance of the bathing solution and the electrodes, $G_s = 10^{-6}\ \Omega^{-1}\cdot cm^{-2}$; the capacitance of the membrane, $C_m = 5\times10^{-7}\ F\cdot cm^{-2}$; the degree of the polyion polymerization, $DP = -100$; the initial flux, $J_0 = 5\times10^{-17}$ mol·s^{-1}·cm^{-2}.

V the polySia flux equals to 6.39×10^{-18} mol·s^{-1}·cm^{-2} (88% decrease) and -1.38×10^{-14} mol·s^{-1}·cm^{-2} (276-fold increase with the inversion of the flux direction) after time $t = 1$ ms and $t = 1$ s, respectively. The calculated decrease of polySia flux corresponds to the measured [4,5] inhibition

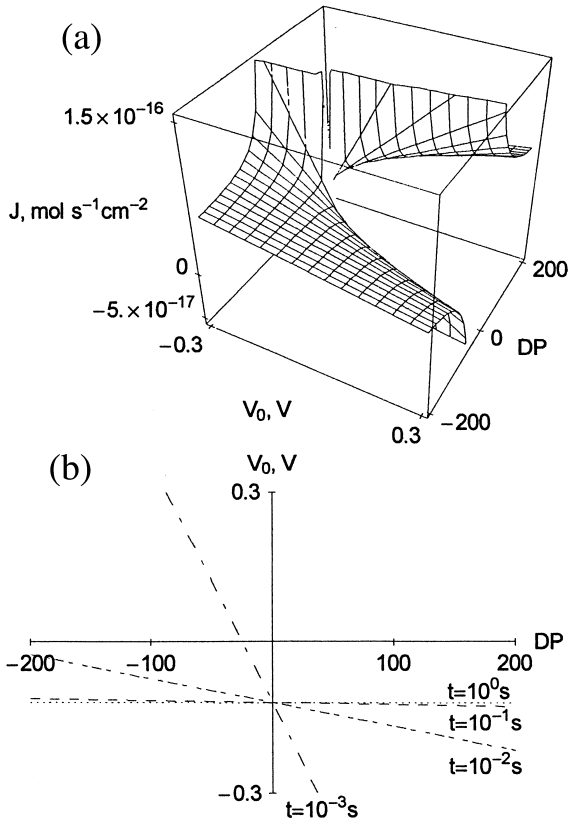

Fig. 3. (a) The dependence of the flux of polyion chains across the membrane, J, on external potential, V_0, and the degree of the polyion polymerization, DP. PolySia is represented by negative values of DP which correspond to the polySia ionic valency. Calculated for: the resting potential of the membrane, $E_r = -0.12$ V; the electrical conductance of the bathing solution and the electrodes, $G_s = 10^{-6}\ \Omega^{-1}\cdot cm^{-2}$; the capacitance of the membrane, $C_m = 5\times10^{-7}\ F\cdot cm^{-2}$; time, $t = 10^{-3}$ s; the electrical conductance of the membrane, $G_m = 10^{-6}\ \Omega^{-1}\cdot cm^{-2}$; the initial flux, $J_0 = 5\times10^{-17}$ mol·s^{-1}·cm^{-2}. (b) The reversal curves obtained from (a) and showing the relationship between the external potential, V_0, and the degree of the polyion polymerization, DP, for the polyion flux, $J = 0$. PolySia is represented by negative values of DP which correspond to the polySia ionic valency. Each line was plotted for different time, t. Calculated for: the resting potential of the membrane, $E_r = -0.12$ V; the electrical conductance of the bathing solution and the electrodes, $G_s = 10^{-6}\ \Omega^{-1}\cdot cm^{-2}$; the capacitance of the membrane, $C_m = 5\times10^{-7}\ F\cdot cm^{-2}$; the electrical conductance of the membrane, $G_m = 10^{-6}\ \Omega^{-1}\cdot cm^{-2}$; the initial flux, $J_0 = 5\times10^{-17}$ mol·s^{-1}·cm^{-2}.

of polySia translocation across the inner bacterial membrane. As presented in Fig. 3a, the polySia flux (after time 1 ms) increases for negative values of external potential with the decrease of polySia chain length with the maximal 32-fold increase: from 5.9×10^{-7} mol·s^{-1}·cm^{-2} (for $V_0=-0.3$ V and $DP=-200$) to 1.9×10^{-15} mol·s^{-1}·cm^{-2} (for $V_0=-0.3$ V and $DP=-1$). For positive values of the external potential the flux decreases with the maximal 153-fold decrease: from 2.8×10^{-17} mol·s^{-1}·cm^{-2} (for $V_0=0.3$ V and $DP=-200$) to -4.3×10^{-15} mol·s^{-1}·cm^{-2} (for $V_0=-0.3$ V and $DP=-1$). The reversal curves evaluated from Fig. 2a and Fig. 3a are presented in Fig. 2b and Fig. 3b for different levels of the membrane conductivity and time, respectively. For the points lying below these curves the polySia flux is positive whereas the points above the curves give the negative polySia flux, i.e. the flux of opposite direction with respect to the initial flux, J_0.

The relationship between the polySia flux and the membrane conductance, and time, for the external potential -0.06 V is presented in Fig. 4. For the membrane conductance equal 10^{-5} Ω^{-1}·cm^{-2} the polySia flux changes from 5×10^{-17} mol·s^{-1}·cm^{-2} ($t=0$), through the value -1.26×10^{-17} mol·s^{-1}·cm^{-2} (the minus sign represents the change to the flux of opposite direction), to the value -2.96×10^{-15} mol·s^{-1}·cm^{-2} ($t=1$ s). It means that there is the 236-fold increase in the flux in the time interval (10^{-3}; 1) s. For the membrane conductance 10^{-8} Ω^{-1}·cm^{-2} the changes in the polySia flux are much smaller: from the value 5×10^{-17} mol·s^{-1}·cm^{-2} ($t=0$), through the value 4.99×10^{-17} mol·s^{-1}·cm^{-2} ($t=1$ ms) to the value -2.09×10^{-17} mol·s^{-1}·cm^{-2} ($t=1$ s).

Fig. 5a shows the polySia flux as a function of the membrane conductance and the degree of polymerization of polySia for time, $t=1$ ms, and the external potential $V_0=-0.06$ V. For $DP=-200$ the flux decreases over 2.5-fold from 4.99×10^{-17} mol·s^{-1}·cm^{-2} to 1.82×10^{-17} mol·s^{-1}·cm^{-2} with the increase of the membrane conductance from 10^{-8} Ω^{-1}·cm^{-2} to 10^{-5} Ω^{-1}·cm^{-2}, respectively. For DP of polySia equal to -10 the changes are much bigger: from the value 4.93×10^{-17} mol·s^{-1}·cm^{-2} to the value -5.66×10^{-16} mol·s^{-1}·cm^{-2}; for $DP=-1$ the corresponding values of polySia flux are 4.37×10^{-17} mol·s^{-1}·cm^{-2} and -6.10×10^{-15} mol·s^{-1}·cm^{-2}. For the points lying below the reversal curves (Fig. 5b), the polySia flux is positive, on the other hand the points above the curves give the negative flux. The reversal curves were plotted for different values of time.

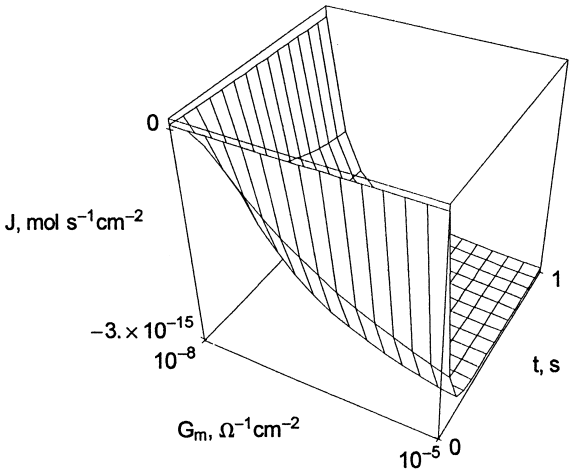

Fig. 4. The dependence of the flux of polyion chains across the membrane, J, on the conductance of the membrane, G_m, and time, t. Calculated for: the external potential, $V_0=-0.06$ V; the resting potential of the membrane, $E_r=-0.12$ V; the electrical conductance of the bathing solution and the electrodes, $G_s=10^{-6}$ Ω^{-1}·cm^{-2}; the capacitance of the membrane, $C_m=5\times10^{-7}$ F·cm^{-2}; the degree of the polyion polymerization, $DP=-100$; the initial flux, $J_0=5\times10^{-17}$ mol·s^{-1}·cm^{-2}.

The dependency of the polySia flux on time and the degree of polySia polymerization for the membrane conductance 10^{-6} Ω^{-1}·cm^{-2} and the external potential -0.06 V, is visualized in Fig. 6a. For long polySia chains (DP equal to -200) the polySia flux decreases in time from the value 5×10^{-17} mol·s^{-1}·cm^{-2} ($t=0$), reaching the values 4.67×10^{-17} mol·s^{-1}·cm^{-2} (a 6.5% decrease) and -9.82×10^{-16} mol·s^{-1}·cm^{-2} (a threefold decrease with the change of the flux into opposite direction) for time equal to 1 ms and 1 s, respectively. For oligoSia chains ($DP=-10$) the decrease is bigger (from 5×10^{-17} mol·

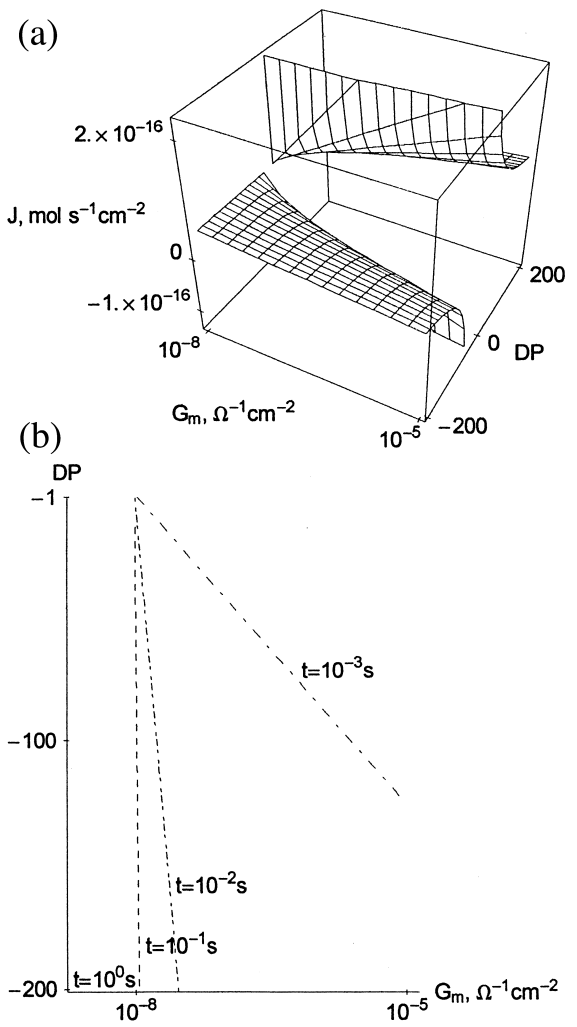

Fig. 5. (a) The dependence of the flux of polyion chains across the membrane, J, on the conductance of the membrane, G_m, and the degree of the polyion polymerization, DP. PolySia is represented by negative values of DP which correspond to the polySia ionic valency. Calculated for: the external potential, $V_0 = -0.06$ V; the resting potential of the membrane, $E_r = -0.12$ V; the electrical conductance of the bathing solution and the electrodes, $G_s = 10^{-6}\ \Omega^{-1}\cdot cm^{-2}$; the capacitance of the membrane, $C_m = 5\times10^{-7}\ F\cdot cm^{-2}$; time, $t = 10^{-3}$ s; the initial flux, $J_0 = 5\times10^{-17}\ mol\cdot s^{-1}\cdot cm^{-2}$. (b) The reversal curves obtained from (a) and showing the relationship between the degree of the polyion polymerization, DP, and the conductance of the membrane, G_m, for the polyion flux, $J = 0$. Each line was plotted for different time, t. Calculated for: the external potential, $V_0 = -0.06$ V; the resting potential of the membrane, $E_r = -0.12$ V; the electrical conductance of the bathing solution and the electrodes, $G_s = 10^{-6}\ \Omega^{-1}\cdot cm^{-2}$; the capacitance of the membrane, $C_m = 5\times10^{-7}\ F\cdot cm^{-2}$; the initial flux, $J_0 = 5\times10^{-17}\ mol\cdot s^{-1}\cdot cm^{-2}$.

$s^{-1}\cdot cm^{-2}$ to $-1.22\times10^{-17}\ mol\cdot s^{-1}\cdot cm^{-2}$ and $-1.97\times10^{-14}\ mol\cdot s^{-1}\cdot cm^{-2}$, respectively. The maximal drop is observed for monomers ($DP = -1$): from $5\times10^{-17}\ mol\cdot s^{-1}\cdot cm^{-2}$ to $-5.71\times10^{-16}\ mol\cdot s^{-1}\cdot cm^{-2}$ and $-1.97\times10^{-13}\ mol\cdot s^{-1}\cdot cm^{-2}$ (over 12-fold decrease in the time interval [0; 10^{-3}] s and 345-fold decrease in the time interval [10^{-3}; 1] s.

The reversal curves obtained from Fig. 6a, for different values of the membrane conductances are presented in Fig. 6b. The area below the curves represents the positive polySia flux (with the same direction as the initial flux J_0) whereas the area above the curves represents the negative polySia flux (with the appropriate direction with comparison with the initial flux J_0.

The steady-state diffusion of ions through separate, selective channels was described according to irreversible thermodynamics [18]. Ion fluxes thus obtained were the same as those in the parallel conductance model. The equivalent electrical circuit for this system had its electromotive forces expressed by the chemical potentials of the diffusing ions. It was concluded that the passive diffusion flows remain steady, since active transport mechanisms pump the ions up their electrochemical potentials. The same equivalent circuit was used to describe the active extraction of anions from the living cell and for explanation of the measured plasma membrane potential of cells, especially when the potential did not behave as the potassium electrode. Membrane potential created in the process of passive diffusion (or at equilibrium) of ions was identified with the so-called pump potential. In contrast to our approach the author analyzed only the fluxes of univalent ions.

Ionic circuit analysis was applied to vesicular systems containing insect midgut transport proteins [14]. In this analysis pumps, porters and channels, as well as ionic concentration gradients and membrane capacitance, were components of ionic circuits that function to transform metabolic energy (e.g. from ATP hydrolysis) into useful metabolic work (e.g. amino acid uptake). Computer-generated time courses of membrane potential reproduced key aspects of the coupling of the proton-motive force generated by an H^+ V-

ATPase to $K^+/2H^+$ antiport and amino acid/K^+ symport in the lepidopteran midgut. Although the authors applied circuit analysis to different experimental conditions they focused on the transmembrane movement of univalent cations and omitted the transport phenomena of polycations or polyanions across biological membranes.

A simple system consisting of a pump for a single ionic species in a membrane separating two aqueous compartments was considered [15]. This analysis departed from all previous ones by representing ionic gradients as charged compartmental capacitances instead of batteries. In the circuit, the ionic (in this case proton) pump was depicted by the pump potential/porter combination, and the frictional and slippage resistances were considered to be negligible and were ignored. In the steady state, in this case equilibrium, the pump generated a proton-motive force which was the product of the pump potential and the proton porter coupling coefficient [15]. The proton-motive force dropped across the series combination of the membrane capacitance and the total proton compartmental capacitance. A vesicular membrane with a proton pump, a porter and counter-ion leakage was also considered, giving a complex electrical equivalent circuit in the case, of both the goblet cell and columnar cell in the midgut epithelium. Similarly to [14] the analysis was done only for univalent ions.

A simple electrical equivalent circuit for the plasmalemma of cells has been shown [19]. The left-hand branch of the circuit represented the passive diffusion of ions across the membrane; the membrane resistance was connected in series with the electromotive force, which is equivalent to the diffusion potential. The right-hand branch represented the electrogenic H^+ pump, which actively transports H^+ ions out of the characean cell. The equation giving the membrane potential for the circuit has been presented [19]. Our analy-

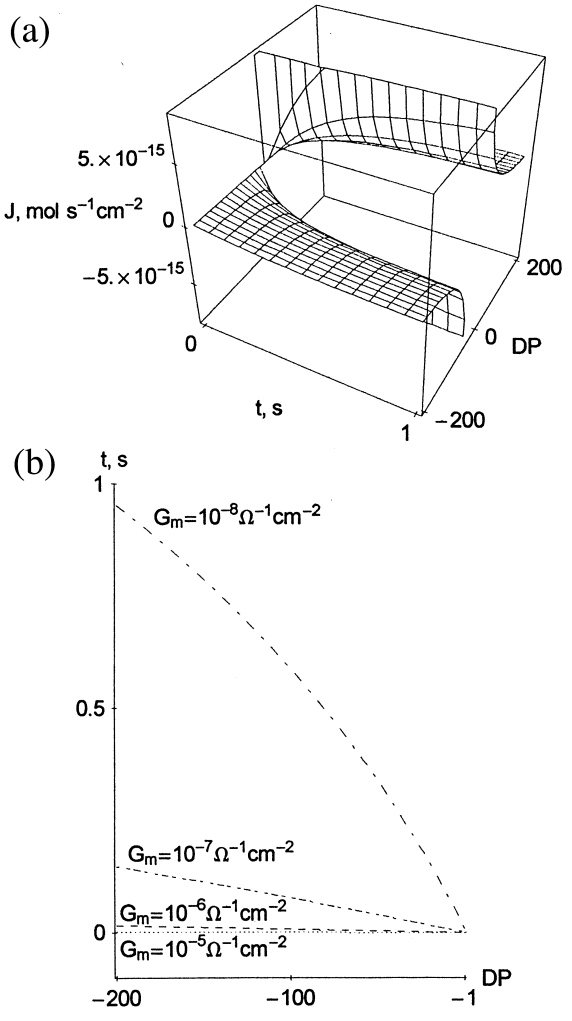

Fig. 6.

Fig. 6(a) The dependence of the flux of polyion chains across the membrane, J, on the degree of the polyion polymerization, DP, and time, t. PolySia is represented by negative values of DP which correspond to the polySia ionic valency. Calculated for: the external potential, $V_0 = -0.06$ V; the resting potential of the membrane, $E_r = -0.12$ V; the electrical conductance of the bathing solution and the electrodes, $G_s = 10^{-6}\ \Omega^{-1}\cdot cm^{-2}$; the capacitance of the membrane, $C_m = 5\times10^{-7}\ F\cdot cm^{-2}$; the electrical conductance of the membrane, $G_m = 10^{-8}\ \Omega^{-1}\cdot cm^{-2}$; the initial flux, $J_0 = 5\cdot 10^{-17}\ mol\cdot s^{-1}\cdot cm^{-2}$. (b) The reversal curves obtained from (a) and showing the relationship between the time, t, and the degree of the polyion polymerization, DP, for the polyion flux, $J = 0$. The lines were plotted for different electrical conductance of the membrane, G_m. Calculated for: the external potential, $V_0 = -0.06$ V; the resting potential of membrane, $E_r = -0.12$ V; the electrical conductance of the bathing solution and the electrodes, $G_s = 10^{-6}\ \Omega^{-1}\cdot cm^{-2}$; the capacitance of the membrane, $C_m = 5\times10^{-7}\ F\cdot cm^{-2}$; the initial flux, $J_0 = 5\times10^{-17}\ mol\cdot s^{-1}\cdot cm^{-2}$.

sis develops this approach for polyion transport and gives solutions in the form of three-dimensional graphs.

The transmembrane potential of biological membranes can be modulated in at least two ways: the first, by using ionophores dissipating the ionic electrochemical potential gradients, and the second, by applying external electrical potential gradient from electrodes placed on opposite sides of the membrane. The modulation of the transmembrane potential by ionophores can be described by using an electrical circuit analogous to the ionic circuit [20]. Both circuits have generators of potential (the battery and the respiratory chain, respectively), both these potentials can be made to perform work and both circuits can be short circuited. The rate of chemical conversion in both the battery and respiratory chain is tightly linked to the current of electrons and ions flowing in the rest of the circuit, which in turn depends on the resistance of the rest of the circuit.

The results of the present paper can describe the experimental results on the influence of ionophores (dissipating the energy of the ionic electrochemical potential gradients) on the translocation of polySia from the cytoplasmic site to the periplasmic site of the *E. coli* K1 inner bacterial membrane [4,5]. In these studies the effect of CCCP — as a modulator of proton transmembrane electrochemical potential gradient ($\Delta\mu_H$), and valinomycin — as a modulator of transmembrane electrical potential gradient ($\Delta\psi$), on the translocation rates were assessed. Spheroplasts derived from RHM 18 strain were labeled during 5 min pulse with [^{14}C]sialic acid, then the transmembrane translocation of sialyl polymers was monitored during a 120-min chase. The presence of both CCCP and valinomycin inhibits polySia translocation rate, in comparison to the control, up to 85 and 50%, respectively. The action of the ionophores on the transmembrane potential of the inner bacterial membrane is analogous to the reduction of the level of the external potential V_0 at time equal zero in the electrical equivalent circuit presented in Fig. 1. In agreement with the experimental analysis, the polySia flux inhibition is observed (Figs. 2 and 3) in the case of when the transmembrane potential decreases.

The present theoretical analysis can also provide a theoretical background for further experimental studies using the voltammetric technique [19,21–25] for analyzing the polyionic fluxes across membranes. In this case, the value of V_0 can be modulated using a potentiostat, the membrane conductance can be determined from the current/voltage characteristics and the relationship between the polyion transmembrane flux and the polyion chain length can be experimentally determined. This technique can also be applied for analysis of polyion translocation events through a single channel/single membrane electropore [26]. If a small piece of membrane with a single channel is considered, the membrane conductance, G_m, [Eq. (12)] can be replaced by the single-channel conductance.

Electrotransfection of cells, i.e. transfection induced by electric field pulses, is an effective technique for introduction of foreign nucleic acid into cells [27]. It was shown that DNA translocation into cells, using a high-voltage pulse, takes less than 3 s, and DNA electrophoresis plays an important role in this process [28]. The authors suggest that the mechanism of cell electrotransfection is underlain by electrophoretic movement of DNA through membrane pores, the rise of which is determined by interaction with DNA in an electric field. Similar to our study, they have investigated the effect of the inversion of the electric field polarity on the translocation rates. They found a 10-fold increase in transfection efficiency with a polarity causing DNA electrophoresis toward the cell, in comparison with the inverse polarity. In accordance to our study (Figs. 3, 5 and 6) they observed the reduction of the translocation rates when the polyanion effective charge was decreased. DNA penetration from T4 phage adsorbed to *E. coli* was measured at different membrane potentials [29]. The authors found that the T4 DNA injection process depended on a minimum V_m below which there was no penetration. This threshold of membrane potential for DNA penetration was independent of ΔpH. In accordance with our relationships, the authors obtained 95% reduction in DNA penetration when the transmembrane potential was re-

duced from 110 to 60 mV using a valinomycin ionophore.

In conclusion, we have shown that the modulation of the transmembrane potential of the bacterial inner membrane of the polySia chain in bacterial cells can be responsible for the changes observed in the transmembrane translocation rate. This analysis describes also the effect of transmembrane potential on the translocation rate of negatively charged polyanionic polynucleotides across membranes. The investigations were extended for the modulation of transmembrane translocation of polycationic homopolymers. These polymers strongly interact with DNA and are used to compact plasmid DNA in order to increase the uptake of foreign genes in mammalian cells with the aim to transfect them [30–32]. The presented analysis can also provide a theoretical background for further experimental studies using the voltammetric technique both at the membrane level and the single-channel/single-electropore level.

Acknowledgements

The authors would like to thank Professor Frederic A. Troy for many helpful discussions. This work was carried out within the research project No. 6 PO4A 014 10 supported by the State Committee for Scientific Research in 1996–1998.

References

[1] U. Rutishauser, L. Landmesse, Polysialic acid in the vertebrate nervous system: a promoter of plasticity in cell-cell interactions, Trends Neurosci. 19 (1996) 422–427.

[2] F. Michon, J. Brisson, H. Jennings, Conformational differences between linear a(2-8)-linked homosialooligosaccarides and the epitope of the group B meningococcal polysaccharide, Biochemistry 26 (1987) 8399–8405.

[3] J.Z. Kiss, G. Rougon, Cell biology of polysialic acid, Curr. Opin. Neurobiol. 7 (1997) 640–646.

[4] F.A. Troy, T. Janas, T. Janas, R.I. Merker, Topology of the poly-α-2,8-sialyltransferase in *E. coli* K1 and energetics of polysialic acid chain translocation across the inner membrane, Glycoconjugate J. 7 (1990) 383.

[5] F.A. Troy, T. Janas, T. Janas, R.I. Merker, Vectorial translocation of polysialic acid chains across the inner membrane of *Escherichia coli* K1, Fed. Am. Soc. Exp. Biol. J. 5 (1991) 6835.

[6] F.A. Troy, Polysialylation: from bacteria to brains, Glycobiology 2 (1992) 5–23.

[7] U. Rutishauser, Polysialic acid at the cell surface: biophysics in service of cell interactions and tissue plasticity, J. Cell Biochem. 70 (1998) 304–312.

[8] G.J. Boulnois, I.S. Roberts, R. Hodge, K.R. Hardy, K.B. Jann, K.N. Timmis, Analysis of the K1 capsule biosynthesis genes of *Escherichia coli*: definition of three functional regions for capsule production, Mol. Gen. Genet. 208 (1987) 242–246.

[9] R.P. Silver, C.W. Finn, W.F. Vann et al., Molecular cloning of the K1 capsular polysaccharide genes of *E. coli*, Nature 289 (1981) 696–698.

[10] A.L. Hodkin, A.F. Huxley, A quantitative description of membrane current and its application to conduction and excitation in nerve, J. Physiol. 117 (1952) 500–544.

[11] L.J. Mullens, K. Noda, The influence of sodium-free solutions on the membrane potential of frog muscle fibers, J. Gen. Physiol. 47 (1963) 117–132.

[12] U. Kishimoto, N. Kami-Ike, Y. Takeuchi, A quantitative expression of the electrogenic pump and its possible role in the excitation of *Chara* internodes, in: W.J. Adleman, D.E. Goldman (Eds.), The Biophysical Approach to Excitable Systems, Plenum Press, New York, 1981, p. 165.

[13] G.A. Gerencser, B.R. Stevens, Thermodynamics of symport and antiport catalyzed by cloned or native transporters, J. Exp. Biol. 196 (1994) 59–75.

[14] F.G. Martin, W.R. Harvey, Ionic circuit analysis of K^+/H^+ antiport and amino acid/K^+ symport energized by a proton-motive force in *Manduca sexta* larval midgut vesicles, J. Exp. Biol. 196 (1994) 77–92.

[15] F.G. Martin, Circuit analysis of transmembrane voltage relationships in V-ATPase-coupled ion movements, J. Exp. Biol. 172 (1992) 387–402.

[16] T.E. Rohr, F.A. Troy, Structure and biosynthesis of surface polymers containing polysialic acid in *Escherichia coli*, J. Biol. Chem. 255 (1980) 2332–2342.

[17] Ch. Weisgerber, F.A. Troy, Biosynthesis of the polysialic acid capsule in *Escherichia coli* K1, J. Biol. Chem. 265 (1990) 1578–1587.

[18] B. Tomicki, Steady-state diffusion and the cell resting potential, Eur. Biophys. J. 28 (1999) 330–337.

[19] Z. Trela, T. Janas, S. Witek, S. Przestalski, Effects of quaternary ammonium salts on membrane potential and electric conductance in internodal cells of *Nitellopsis obtusa*, Physiol. Plant. 78 (1990) 57–60.

[20] D.G. Nicholls, Bioenergetics, Academic Press, New York, 1982.

[21] T. Janas, H.T. Tien, Influence of dolichyl phosphate on permeability and stability of bilayer lipid membranes, Biochim. Biophys. Acta 939 (1988) 624–628.

[22] T. Janas, J. Kuczera, T. Chojnacki, Voltammetric analy-

sis of polyisoprenoid-containing bilayer lipid membranes, Chem. Phys. Lipids 51 (1989) 227–238.
[23] T. Janas, T. Janas, Interaction of undecaprenyl phosphate with phospholipid bilayers, Chem. Phys. Lipids 77 (1995) 89–97.
[24] T. Janas, K. Walinska, T. Janas, Electroporation of polyprenol-phosphatidylcholine bilayer lipid membranes, Bioelectrochem. Bioenerg. 45 (1998) 215–220.
[25] T. Janas, T. Janas, K. Walinska, The effect of hexadecaprenyl diphosphate on phospholipid membranes, Biochim. Biophys. Acta 1464 (2000) 273–283.
[26] N.I. Hristova, I. Tsoneva, E. Neumann, Sphingosine-mediated electroporative DNA transfer through lipid bilayers, FEBS Lett. 415 (1997) 81–86.
[27] T.-D. Xie, L. Sun, T.Y. Tsong, Study of mechanisms of electric field-induced DNA transfection. DNA entry by surface binding and diffusion through membrane pores, Biophys. J. 58 (1990) 13–19.
[28] V.A. Klenchin, S.I. Sukharev, S.M. Serov, L.V. Chernomordik, Y.A. Chizmadzhev, Electrically induced DNA uptake by cells is a fast process involving DNA electrophoresis, Biophys. J. 60 (1991) 804–811.
[29] B. Labedan, K.B. Heller, A.A. Jasaitis, T.H. Wilson, E.B. Goldberg, A membrane potential threshold for phage T4 DNA injection, Biochim. Biophys. Res. Commun. 93 (1980) 625–630.
[30] M. Zenke, P. Steinlein, E. Wagner, M. Cotten, H. Beug, M.L. Birnstiel, Receptor-mediated endocytosis of transferrin-polycation conjugates: an efficient way to introduce DNA into hematopoietic cells, Proc. Natl. Acad. Sci. USA 87 (1990) 3655–3659.
[31] T.B. Wymn, F. Nicol, O. Zelphati, P.V. Scaria, C. Plank, F.C. Szoka, Design, synthesis and characterization of a cationic peptide that binds to nucleic acids and permeabilizes bilayers, Biochemistry 36 (1997) 3008–3017.
[32] P. Midoux, M. Monsigny, Efficient gene transfer by histidylated polylysine/pDNA complexes, Bioconjugate Chem. 10 (1999) 406–411.